

# Epileptic Seizure Prediction Based on Multivariate Statistical Process Control of Heart Rate Variability Features

Koichi Fujiwara\*, *Member, IEEE*, Miho Miyajima, Toshitaka Yamakawa, *Member, IEEE*, Erika Abe, *Member, IEEE*, Yoko Suzuki, Yuriko Sawada, Manabu Kano, *Member, IEEE*, Taketoshi Maehara, Katsuya Ohta, Taeko Sasai-Sakuma, Tetsuo Sasano, Masato Matsuura, and Eisuke Matsushima

**Abstract—Objective:** The present study proposes a new epileptic seizure prediction method through integrating heart rate variability (HRV) analysis and an anomaly monitoring technique. **Methods:** Because excessive neuronal activities in the preictal period of epilepsy affect the autonomic nervous systems and autonomic nervous function affects HRV, it is assumed that a seizure can be predicted through monitoring HRV. In the proposed method, eight HRV features are monitored for predicting seizures by using multivariate statistical process control, which is a well-known anomaly monitoring method. **Results:** We applied the proposed method to the clinical data collected from 14 patients. In the collected data, 8 patients had a total of 11 awakening preictal episodes and the total length of interictal episodes was about 57 h. The application results of the proposed method demonstrated that seizures in ten out of eleven awakening preictal episodes could be predicted prior to the seizure onset, that is, its sensitivity was 91%, and its false positive rate was about 0.7 times per hour. **Conclusion:** This study proposed a new HRV-based epileptic seizure prediction method, and the possibility of realizing an HRV-based epileptic seizure prediction system was shown. **Significance:** The proposed method can be used in daily life, because the heart rate can be measured easily by using a wearable sensor.

**Index Terms—Epilepsy, heart rate variability analysis, multivariate statistical process control (MSPC), seizure prediction.**

## I. INTRODUCTION

**E**PILEPSY is a diverse set of chronic neurological disorders characterized by seizures, and about 1% of people worldwide have epilepsy [1]. Although epileptic seizures can be usually controlled with appropriate medications, about 30% of epileptic patients do not have seizure control even if they use the best available medications [2].

Manuscript received May 1, 2015; revised December 3, 2015; accepted December 16, 2015. Date of publication December 24, 2015; date of current version May 18, 2016. This work was supported in part by JSPS KAKENHI 25282175, the SEI Group CSR Foundation, the Japan Prize Foundation, the Japan Epilepsy Research Foundation, and the Mitsubishi Foundation. *Asterisk indicates corresponding author.*

\*K. Fujiwara is with the Department of Systems Science, Kyoto University, Kyoto 606-8501, Japan (e-mail: fujiwara.koichi@i.kyoto-u.ac.jp).

E. Abe and M. Kano are with the Department of Systems Science, Kyoto University.

Y. Suzuki, Y. Sawada, M. Miyajima, T. Maehara, K. Ohta, T. Sasano, M. Matsuura, and E. Matsushima are with the Tokyo Medical and Dental University.

T. Yamakawa is with the Kumamoto University.

T. S. Sasai is with the Tokyo Medical University.

Color versions of one or more of the figures in this paper are available online at <http://ieeexplore.ieee.org>.

Digital Object Identifier 10.1109/TBME.2015.2512276

Convulsions or loss of consciousness associated with uncontrolled seizures may cause serious injuries not only for patients themselves but also for people around them. If patients can be given a warning before the seizure onset, their quality of life (QoL) may be improved because their safety can be ensured.

Closed-loop seizure treatment systems have been proposed, which consist of two parts: seizure prediction and automatic seizure treatment. These systems automatically give a warning to caretakers or hospitals, or switch ON a neurostimulator implanted in a patient for normalizing brain activities, when a seizure is predicted [3]. An accurate seizure prediction method is needed for realizing such systems.

Epileptic seizure prediction based on the electroencephalogram (EEG) has been studied [4], [5]. However, the use of EEG in daily life is not realistic because EEG recording strongly puts restrictions on the body and is intolerant to artifacts.

On the other hand, epileptic seizures can lead to changes in cardiac autonomic nervous function affecting both sympathetic and parasympathetic nervous systems [6], [7]. The activation of central autonomic nervous system by epileptic discharge propagation during a seizure is thought to be responsible for the preictal cardiac autonomic symptoms [8]. Ictal tachycardia and bradycardia are well-known autonomic phenomena associated with epileptic seizures, and such cardiac changes occur not only at the same time as but also prior to the EEG seizure onset [9], [10].

The RR interval (RRI) fluctuation in an electrocardiogram (ECG), called heart rate variability (HRV), is a well-known phenomenon which reflects the autonomic nervous function [11], and changes in HRV in preictal phase have been reported [12], [13]. In addition, seizure detection based on HRV has been attempted [14]. This method was able to detect seizures by using the Lorentz plot; however, seizures of only three out of 17 patients could be detected before their onset. A new methodology for predicting an epileptic seizure needs to be developed.

Another problem of HRV-based epileptic seizure prediction is developing an RRI measurement device that can be used in daily life. Although the Holter monitor has been used to measure long-term RRI, its home-use is difficult because the Holter monitor is expensive and requires operation skills. Yamakawa *et al.* developed a wearable RRI sensor, which can measure RRI without any special skills and be manufactured for less than US \$ 100 [15]. If an HRV-based seizure detection method can

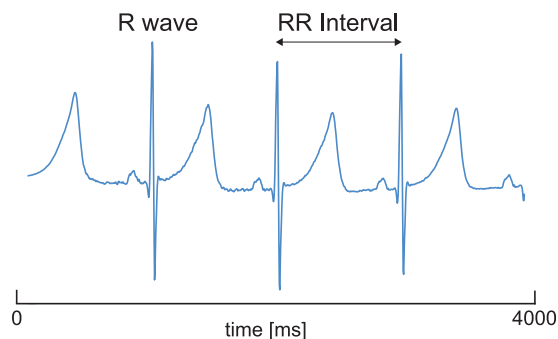


Fig. 1. Example of a typical ECG.

be implemented in such a device, a wearable epileptic seizure prediction system becomes available.

The present study proposes a new HRV-based epileptic seizure prediction method for realizing a seizure prediction device that can be used in daily life. The proposed method consists of two parts: HRV feature extraction from RRI data of epileptic patients, and epileptic seizure prediction by utilizing an anomaly monitoring technique whose inputs are the extracted HRV features. Multivariate statistical process control (MSPC) [16]–[18], which is a well-known anomaly monitoring method, is used for the epileptic seizure prediction.

This paper is organized as follows. Section II introduces HRV analysis, and a new seizure prediction method is proposed by integrating HRV analysis and MSPC in Section III. Section IV reports application results of the proposed method to clinical data and discusses the results. The conclusion and future work are described in Section V.

## II. HRV ANALYSIS

Since HRV reflects autonomic nervous activities, HRV analysis has been used for monitoring stress, drowsiness, and cardiovascular disease [19]–[22]. In this section, the HRV features used for seizure prediction are explained briefly.

### A. RR Interval

A typical ECG trace of the cardiac cycle (standard lead II) consists of some peaks as shown in Fig. 1, and the highest peak is called the R wave. The RRI [ms] is defined as the interval between an R wave and the next R wave.

A part of the raw RRI data collected from a healthy person is shown in Fig. 2(a). Since the raw RRI data are not sampled at equal intervals, frequency domain features cannot be extracted. Thus, the raw RRI data are interpolated by using spline and resampled at equal intervals. Fig. 2(b) shows the resampled RRI data whose sampling interval is 1 s.

### B. Time Domain Features

The following time domain features can be calculated from the original RRI data [19].

- 1) **meanNN**: Mean of RRI.
- 2) **SDNN**: Standard deviation of RRI.
- 3) **RMSSD**: Root mean square of difference of adjacent RRI.
- 4) **Total Power (TP)**: Variance of RRI.

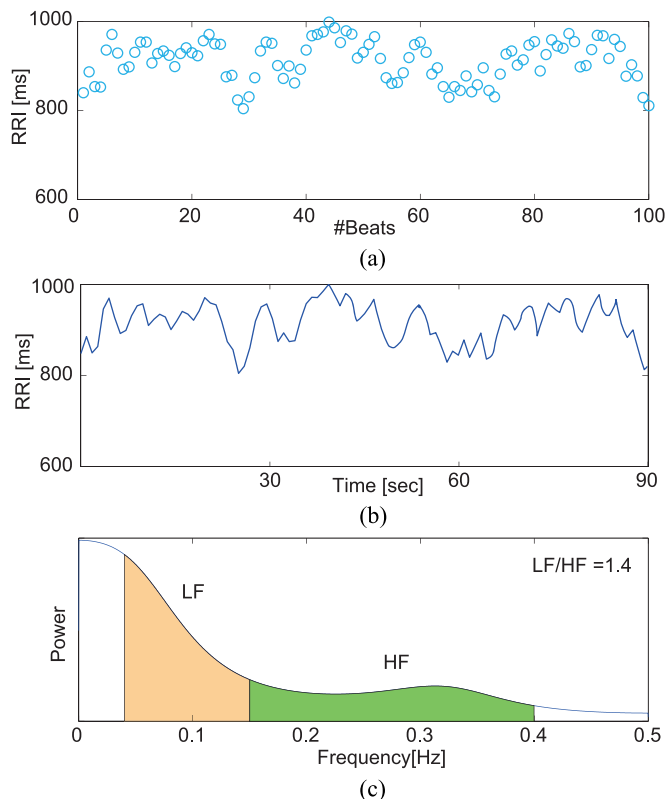


Fig. 2. Example of RRI data analysis: (a) the raw RRI data, (b) the resampled RRI data and (c) the PSD and its LF/HF.

- 5) **NN50**: The number of pairs of adjacent RRI whose difference is more than 50 ms within a given length of measurement time.

### C. Frequency Domain Features

The following frequency domain features can be obtained from the power spectrum density (PSD) of the resampled RRI data, and the PSD can be calculated by using Fourier analysis or an autoregressive (AR) model [19].

- 1) **LF**: Power of the low frequency band (0.04–0.15 Hz) in a PSD. LF reflects both the sympathetic and parasympathetic activity nervous systems activity.
- 2) **HF**: Power of the high frequency band (0.15–0.4 Hz) in a PSD. HF reflects the parasympathetic nervous system activity.
- 3) **LF/HF**: Ratio of LF to HL. LF/HF expresses the balance of the sympathetic nervous system activity with the parasympathetic nervous system activity.

Fig. 2(c) shows the PSD and its LF/HF of the resampled RRI data shown in Fig. 2(b). According to the HRV analysis guideline, the RRI data should be measured for 2 to 5 min for frequency analysis [19].

## III. EPILEPTIC SEIZURE PREDICTION

Since seizure prediction can be formulated as an anomaly detection problem, the present study uses MSPC, which is a useful statistical technique for detecting anomalies in

multivariate systems, and it has been widely used in many manufacturing processes [16]–[18].

### A. Data Preprocessing

The proposed epileptic seizure prediction method uses eight HRV features described in Section II as input variables, and they are extracted from RRI data.

In HRV feature extraction, a rectangular moving window is used and the window size is 3 min. The time domain features can be extracted directly from the raw RRI data. For frequency domain feature extraction, the RRI data need to be resampled so that its sampling points are arranged at equal intervals. In this study, the third-order spline is used for RRI interpolation, and the sampling rate is 1 Hz. Since HRV reflects blood pressure change and respiration change and their cycles are 10 s and 3–4 s, respectively, HRV is usually less than 0.5 Hz [19]. That is, 1 Hz sampling is enough for frequency domain analysis according to the sampling theorem. This point is discussed in Section IV-E. In addition, an AR model of order ten was used to calculate frequency domain features.

For precise seizure prediction, appropriate HRV preprocessing is needed since HRV has large individuality between patients. For example, the mean heart rate is different for every person and it also changes with age. To cope with individuality in HRV, normalized frequency domain features have been proposed [23]. LF normalized unit (LFnu) and HF normalized unit (HFnu) are defined as follows:

$$\text{LFnu} = \text{LF}/\text{TP} \quad (1)$$

$$\text{HFnu} = \text{HF}/\text{TP}. \quad (2)$$

The present study uses LFnu and HFnu instead of LF and HF. On the other hand, in order to emphasize important HRV features for seizure prediction, any weighted function can be introduced; however, such a weighted function is not used here, because it is difficult to determine which HRV features should be emphasized and which type of weighted function is appropriate for seizure prediction, and the dimensionality of HRV features can be reduced by using principal component analysis (PCA), which is a tool for data compression and information extraction.

Finally, each HRV feature is standardized with zero mean and a standard deviation of one for analysis.

In the following sections, the  $n$ th sampling of HRV features can be denoted by  $\mathbf{x}_n = [x_{n,1}, x_{n,2}, \dots, x_{n,M}]^T$  where  $x_{n,m}$  is the  $n$ th sampling of any  $m$ th HRV feature, where  $M = 8$  in this study because the number of HRV features used for seizure prediction is eight. In addition,  $\mathbf{X} \in \mathbb{R}^{N \times M}$  is a matrix whose  $n$ th row is  $\mathbf{x}_n^T$ .

### B. Multivariate Statistical Process Control

MSPC can detect anomalies that cannot be detected by monitoring each variable independently, because it models the correlation among variables with PCA, which finds linear combinations of variables that describe major trends in a dataset. That is, MSPC detects a sample that does not follow the major trend in the modeling data as an anomaly. In MSPC, the normal

operating condition is defined by two monitored indexes, i.e., the  $T^2$  and  $Q$  statistics [24].

Given a normal data matrix  $\mathbf{X} \in \mathbb{R}^{N \times M}$  whose  $i$ th row is the  $i$ th sample  $\mathbf{x}_i \in \mathbb{R}^M$ , samples are preprocessed appropriately. The singular value decomposition of  $\mathbf{X}$  is as follows:

$$\begin{aligned} \mathbf{X} &= \mathbf{U}\mathbf{\Sigma}\mathbf{V}^T \\ &= [\mathbf{U}_R \quad \mathbf{U}_0] \begin{bmatrix} \mathbf{\Sigma}_R & \mathbf{0} \\ \mathbf{0} & \mathbf{\Sigma}_0 \end{bmatrix} [\mathbf{V}_R \quad \mathbf{V}_0] \end{aligned} \quad (3)$$

where  $\mathbf{U}$  is the left singular matrix,  $\mathbf{\Sigma}$  is the diagonal matrix whose diagonal elements are singular values, and  $\mathbf{V}$  is the right singular matrix. In the PCA, the loading matrix  $\mathbf{V}_R \in \mathbb{R}^{M \times R}$  is derived as the right singular matrix of  $\mathbf{X}$ . The column space of  $\mathbf{V}_R$  is the subspace spanned by principal components and it expresses the correlation among variables. Here,  $M$ ,  $N$ , and  $R (\leq M)$  denote the number of variables, samples, and principal components retained in the PCA model, respectively.

The score is a projection of  $\mathbf{X}$  onto the subspace spanned by principal components. The score matrix  $\mathbf{T}_R \in \mathbb{R}^{N \times R}$  is given by

$$\mathbf{T}_R = \mathbf{X}\mathbf{V}_R. \quad (4)$$

$\mathbf{X}$  can be reconstructed or estimated from  $\mathbf{T}_R$  with linear transformation  $\mathbf{V}_R$ ,

$$\hat{\mathbf{X}} = \mathbf{T}_R\mathbf{V}_R^T = \mathbf{X}\mathbf{V}_R\mathbf{V}_R^T. \quad (5)$$

The information lost by the dimensional compression, that is, errors, is written as

$$\mathbf{E} = \mathbf{X} - \hat{\mathbf{X}} = \mathbf{X}(\mathbf{I} - \mathbf{V}_R\mathbf{V}_R^T). \quad (6)$$

Using the errors, the  $Q$  statistic is defined as

$$\begin{aligned} Q &= \sum_{m=1}^M (x_m - \hat{x}_m)^2 \\ &= \mathbf{x}^T (\mathbf{I} - \mathbf{V}_R\mathbf{V}_R^T) \mathbf{x} \end{aligned} \quad (7)$$

where  $\mathbf{x}$  is a sample. The  $Q$  statistic is the squared distance between the sample and the subspace spanned by principal components. In other words, the  $Q$  statistic is a measure of dissimilarity between the sample and the modeling data from the viewpoint of the correlation among variables.

In addition, to monitor anomalies on the subspace spanned by principal components, Hotelling's  $T^2$  statistic is used. The  $T^2$  statistic is defined as

$$\begin{aligned} T^2 &= \sum_{r=1}^R \frac{t_r^2}{\sigma_{t_r}^2} \\ &= \mathbf{x}^T \mathbf{V}_R \mathbf{\Sigma}_R^{-2} \mathbf{V}_R^T \mathbf{x} \end{aligned} \quad (8)$$

where  $\sigma_{t_r}$  denotes the standard deviation of the  $r$ th score  $t_r$ . The  $T^2$  statistic expresses the Mahalanobis distance from the origin in the subspace spanned by principal components. When the  $T^2$  statistic is small, the sample is close to the mean of the modeling data. MSPC detects an anomaly when either the  $T^2$  or  $Q$  statistic exceeds the predefined control limit.

The number of principal components  $R$  has to be determined carefully as a tuning parameter. When  $R$  is small, the PCA model cannot capture important data trends and this leads to a deterioration in the anomaly detection performance. On the other hand, since PCA models noisy data variance as well as normal data variance when  $R$  is large, it increases false positives (FPs). Although it is difficult to determine  $R$  appropriately, the cumulative proportion of principal components can be used for its tuning. The proportion of the  $r$ th principal component  $C_r$  is as follows:

$$C_r = \frac{\sigma_{t_r}^2}{\sum_{m=1}^M \sigma_{t_m}^2}. \quad (9)$$

$C_r$  shows the rate of the data represented by the  $r$ th principal component in the original data. The cumulative proportion until the  $r$ th principal component is defined as follows:

$$P_r = \sum_{m=1}^r C_r = \frac{\sum_{m=1}^r \sigma_{t_m}^2}{\sum_{m=1}^M \sigma_{t_m}^2}. \quad (10)$$

Using  $P_r$ , the number of principal components  $R$  can be determined so that  $P_r$  reaches the predefined value, such as 80% or 90%.

The control limits, for example, can be determined as  $\alpha\%$  confidence limits. In other words, they are set so that  $\alpha\%$  of samples representing the normal condition are below the control limits, and the other  $(100 - \alpha)\%$  are above them. The control limits become large as  $\alpha$  becomes large. That is,  $\alpha$  controls the sensitivity and the specificity of MSPC, and usually the 99% or 95% confidence limits are adopted.

In seizure prediction, the interictal RRI data and the preictal RRI data are defined as normal data and anomalous data, respectively. It is difficult to collect a sufficient number of preictal RRI data from epileptic patients, and collecting the interictal RRI data and the RRI data of healthy people is much easier than preictal RRI data collection. Although, in general, both normal and anomalous data are needed for modeling, MSPC requires only normal data, which is one of its advantages.

### C. Seizure Prediction

The present study proposes a new seizure prediction method, in which the HRV features are extracted from the RRI data measured from epileptic patients, and the extracted HRV features are monitored by using MSPC.

Before prediction, the interictal RRI data of epileptic patients are analyzed for preparation. The procedure described in Algorithm 1 is adopted.

In this procedure,  $\mathbf{y}^{\{i\}}$  is the interictal RRI data recorded from the  $i$ th patient and  $I$  is the number of patients. First, interictal HRV features are extracted from  $\mathbf{y}^{\{i\}}$ , and these HRV features are merged into one matrix and preprocessed in steps 1–5. The singular value matrix  $\Sigma_R$  and the loading matrix  $\mathbf{V}_R$  are derived from the preprocessed HRV data matrix for calculating the  $T^2$  and  $Q$  statistics in step 6. At this time, the number of principal components  $R$  has to be selected carefully for precise seizure prediction. Finally, their control limits have to be determined for each patient in steps 7–9.

---

#### Algorithm 1 Preparation of seizure prediction

---

- 1: **for all**  $i$  such that  $1 \leq i \leq I$  **do**
  - 2:   Extract the  $i$ th patient interictal HRV features  $\tilde{\mathbf{X}}^{\{i\}}$  from  $\mathbf{y}^{\{i\}}$ .
  - 3: **end for**
  - 4: Merge matrixes  $\tilde{\mathbf{X}}^{\{1\}}, \dots, \tilde{\mathbf{X}}^{\{I\}}$  into one matrix  $\tilde{\mathbf{X}}$ .
  - 5: Preprocess  $\tilde{\mathbf{X}}$  appropriately, and it is referred to as  $\mathbf{X}$ .
  - 6: Derive  $\Sigma_R$  and  $\mathbf{V}_R$  from  $\mathbf{X}$  through singular value decomposition.
  - 7: **for all**  $i$  such that  $1 \leq i \leq I$  **do**
  - 8:   Define the control limits of the  $T^2$  and  $Q$  statistics for the  $i$ th patient,  $\bar{T}^2\{i\}$  and  $\bar{Q}\{i\}$ .
  - 9: **end for**
- 

---

#### Algorithm 2 Seizure prediction

---

- 1: set  $\tau[0] \leftarrow 0, C[0] \leftarrow \mathcal{N}$ .
  - 2: **while do**
  - 3:   Collect the newly measured  $t$ th RRI  $y[t]$ .
  - 4:   Extract the HRV features  $\tilde{\mathbf{x}}[t]$ .
  - 5:   Preprocess  $\tilde{\mathbf{x}}[t]$ , and it is denoted as  $\mathbf{x}[t]$ .
  - 6:   Calculate the  $t$ th  $T^2$  and  $Q$  statistics,  $T^2[t]$  and  $Q[t]$  from  $\mathbf{x}[t]$  by using (7) and (8).
  - 7:   **if**  $((T^2[t] > \bar{T}^2 \vee Q[t] > \bar{Q}) \wedge C[t-1] = \mathcal{N}) \vee ((T^2[t] \leq \bar{T}^2 \wedge Q[t] \leq \bar{Q}) \wedge (C[t-1] = \mathcal{P}))$  **then**
  - 8:      $\tau[t] = \tau[t-1] + y[t]$ .
  - 9:   **else**
  - 10:      $\tau[t] = 0$ .
  - 11:   **end if**
  - 12:   **if**  $\tau[t] \geq \bar{\tau}$  **then**
  - 13:      $C[t] = \neg C[t-1]$  and  $\tau[t] = 0$ .
  - 14:   **end if**
  - 15:   Wait until the next RRI data  $y[t+1]$  is measured.
  - 16: **end while**
- 

The proposed seizure prediction algorithm discriminates the patient status between “preictal” and “interictal,” where “preictal” means an epileptic seizure will occur in the near future. Before seizure prediction starts, the initial RRI data of an epileptic patient have to be stored for more than the window size  $W$ , because HRV feature extraction requires RRI data whose length is  $W$ . After the initial RRI data collection, seizures can be monitored by following Algorithm 2.

In this algorithm,  $y[t] \in \mathfrak{R}$  denotes the  $t$ th RRI and  $t$  denotes the number of sampling from the prediction start.  $\tau$  is a time counter variable and  $C$  expresses the binary patient status  $C = \{\mathcal{N}, \mathcal{P}\}$  where  $\mathcal{N}$  and  $\mathcal{P}$  are “interictal” and “preictal,” respectively. That is,  $\neg \mathcal{N} = \mathcal{P}$  and vice versa.

When either the  $T^2$  or  $Q$  statistic exceeds its control limit for more than the predefined period  $\bar{\tau}$  continuously, the patient status is determined as “preictal,” because the  $T^2$  and  $Q$  statistics can easily fluctuate due to ECG artifacts. Conversely, to change the patient status from “preictal” to “interictal,” both statistics have to stay below their control limits for more than  $\bar{\tau}$  continuously. Steps 7–14 discriminate the patient status, and the patient

TABLE I  
PATIENTS DEMOGRAPHIC AND CLINICAL CHARACTERISTICS

Patient	Sex	Age	Epilepsy syndromes	Medication* [mg/day]
A	male	25	right frontal lobe epilepsy	CBZ 800
B	male	30	left temporal lobe epilepsy	CBZ 400, CLB 10
C	male	14	right occipital, parietal, temporal lobe epilepsy	TPM 550, PHT 250, CLB 20, LTG 400
D	male	24	left frontal lobe epilepsy	LEV 2000, CBZ 500
E	female	31	left mesial temporal lobe epilepsy	PHT 225, TPM 200, CBZ 600, VPA 1200, ZNS 300
F	female	26	left occipital lobe epilepsy	PHT100, LEV 500
G	male	41	right temporal lobe epilepsy	CLB 10, LEV 2000, VPA 800
H	female	39	frontal lobe epilepsy	VPA 50, LEV 250
I	male	20	right temporal lobe epilepsy	CBZ 200, LEV 2000
J	male	43	left temporal lobe epilepsy	ZNS 300, LTG 40
K	male	24	right parietal lobe epilepsy	CBZ 600, LEV 3000, CLB 10, LTG 50
L	male	21	right temporal lobe epilepsy	CBZ 800, LTG 200
M	male	63	left temporal lobe epilepsy	CBZ 200, VPA 400, DZP 5
N	female	27	right frontal lobe epilepsy	LEV 2000

\*VPA: valproic acid, LEV: levetiracetam, CZP: clonazepam, CBZ: carbamazepine, ZNS: zonisamide, TPM: topiramate, CLB: clobazam, PHT: phenytoin, LTG: lamotrigine, GBP: gabapentin, DZP: diazepam

TABLE II  
COLLECTED EPISODES

Patient	Interictal		Preictal	
	Episode	Length [h]	Episode	Length [h]
A**	A1, A2	2.3	As1 – As3	2.1
B**	B1, B2	3.0	Bs1	0.7
C	C1 - C3	2.0	–	–
D	D1 - D6	5.3	–	–
E	E1 - E7	7.5	Es1	0.7
F	F1 - F3	1.9	Fs1, Fs2	1.4
G	G1 - G7	6.0	Gs1	0.7
H	H1 - H7	4.0	–	–
I	I1 - I3	1.7	Is1	0.7
J	J1 - J11	12.7	Js1	0.7
K	K1 - K3	3.6	Ks1	0.7
L	L1 - L6	4.7	–	–
M	M1, M2	2.5	Ms1 – Ms4	2.8
N	N1, N2	0.8	Ns1	0.7
Total		58.0		11.0

\*\* Seizures occurred during sleep.

can be given a warning when the algorithm predicts a seizure in the near future, that is,  $C = P$ .

#### IV. APPLICATION TO CLINICAL DATA

This section reports actual application results of the proposed seizure prediction method to clinical data.

##### A. Data Collection

The clinical data of patients with refractory epilepsy were collected prospectively or retrospectively from patients admitted to the Department of Neurosurgery of Medical Hospital of Tokyo Medical and Dental University (TMDU), the Department of Psychiatry of the National Center of Neurology and Psychiatry (NCNP) hospital, and the Department of Epileptology of the Tohoku University Hospital (TUH) for clinical video-EEG monitoring for presurgical evaluation or assessment of seizure. These prospective and retrospective evaluations of clinically acquired data were approved by the Medical Research Ethics

Committee of TMDU, NCNP, and TUH. Written informed consent was obtained from each participant who was involved in the prospective evaluation.

The video, ECG, and EEG data of patients were simultaneously recorded for about 24–72 h by using a long-term video-EEG monitoring system (Neurofax EEG-1200, NIHON KOHDEN). These tests were conducted in the epilepsy monitoring unit, and the sampling frequency of ECG and EEG was 500 or 1000 Hz. ECG data containing strong artifacts or arrhythmia were eliminated. In this study, a clinical seizure onset is defined as a time point when clinical epileptic seizure manifestation occurs, such as convulsion, automatism, and alteration of consciousness. Two clinical epilepsy specialists, certified by the Japan Epilepsy Society, determined a clinical seizure onset by consulting the seizure video and the EEG data.

The clinical datasets were collected from 14 epileptic patients A–N with localization-related epilepsy. Tables I and II show patient profiles and their collected episodes, respectively. Medication in Table I means the anticonvulsant dosage [mg/day] on the inspection day, and length in Table II denotes the total recorded length [h] of the collected episodes. Unfortunately, the preictal episodes of patients C, D, H, and L could not be recorded.

The data 15 min before and 5 min after seizure onsets were stored as preictal episodes. The data recorded during periods apart from at least 50 min from seizure onsets were defined as interictal episodes. In addition, a clinical technologist determined sleep stages during interictal periods based on the EEG data, and the interictal data during sleep were eliminated because HRV is affected by sleep stage transition and microarousal [25], [26].

On the other hand, in order to validate whether or not the proposed method can predict seizures during sleep, some preictal episodes during sleep, As1–As3 and Bs1, were also evaluated independently from awakening preictal episodes. The epilepsy types of patients A and B were frontal lobe epilepsy (FLE) and temporal lobe epilepsy (TLE), respectively. In FLE, seizures frequently occur during sleep, whereas temporal seizures occur during both wakefulness and sleep in TLE [27], [28].

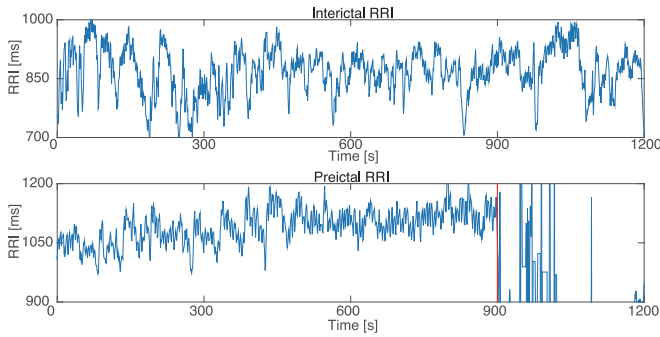


Fig. 3. Obtained RRI data of A2 (top) and As3 (bottom).

The total numbers of collected awakening and sleeping preictal episodes and interictal episodes used for analysis were 11, 4, and 64, respectively.

### B. RRI Data and HRV Features

The R waves in the collected ECG datasets were detected by using a first derivative-based peak detection algorithm, and each RRI was calculated. The obtained raw RRI data of patients A, I, M, and N recorded in interictal and preictal periods are shown in Figs. 3–6. In these figures, a vertical line denotes the seizure onset. Although these figures show that patients experienced sudden tachycardia after the seizure onset, it was difficult to calculate RRI during seizures due to large ECG artifacts because seizures often have dramatic clinical manifestations including posturing, hypermotor automatisms, and ambulation, which cause ECG artifacts. That is, the RRI data after the seizure onset were not reliable.

Eight HRV features described in Section II were extracted by following the procedure in Section III-A. Figs. 7–14 are the obtained HRV features of the RRI data shown in Figs. 4–6. The preictal HRV data show that almost all features, in particular frequency domain features, changed before the seizure onset, while the interictal HRV features did not fluctuate so much.

On the other hand, for example, LF between 200–600 s and LF/HF around 600 s of episode M2 greatly changed as shown in Fig. 11; nevertheless this episode did not contain seizures. According to its RRI data, patient I experienced tachycardia during these periods.

These results indicate that it is difficult to predict seizures by monitoring changes in respective HRV features, and that relationships between multiple features should be monitored.

### C. Prediction Preparation

Seizure prediction was prepared by following Algorithm 1. The HRV features derived from 22 interictal episodes summarized in Table III were used for modeling. The total recorded length of the analyzed episodes was about 18.9 h.

All HRV features calculated in Section IV-B were used as inputs. To cope with individuality between patients, LFnu and HFnu were used instead of LF and HF. In the MSPC, the number of retained principal components  $R$  was determined so that the cumulative proportion reached more than 90%, and  $R = 6$ . The

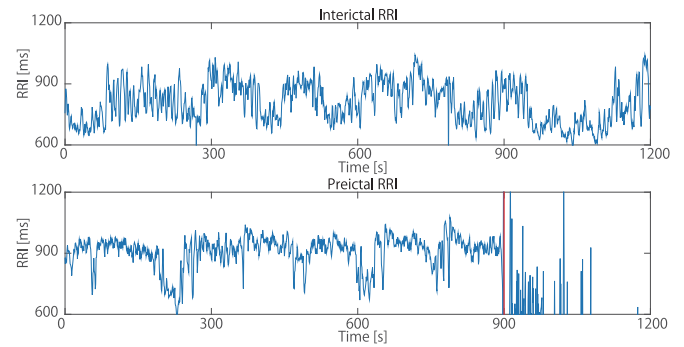


Fig. 4. Obtained RRI data of I3 (top) and Is1 (bottom).

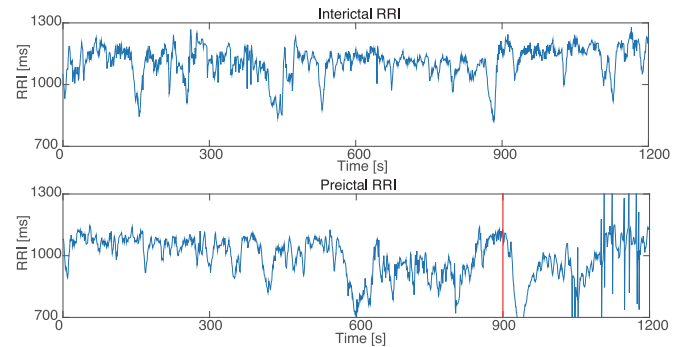


Fig. 5. Obtained RRI data of M2 (top) and Ms2 (bottom).

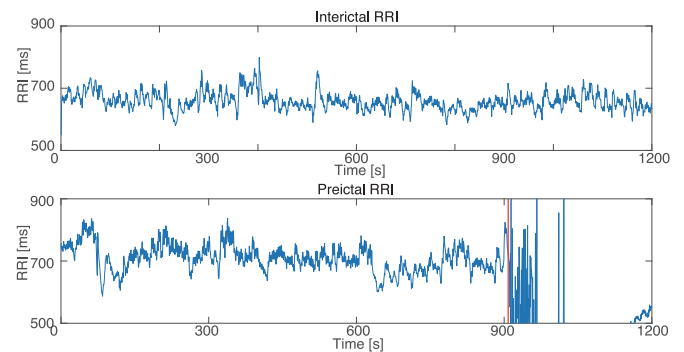


Fig. 6. Obtained RRI data of N2 (top) and Ns1 (bottom).

control limits of the  $T^2$  and  $Q$  statistics were defined for each patient so that they represent 99% confidence limits, i.e., 99% of the interictal data of each patient were recognized as “interictal.” This 99% confidence limit is a common setting in anomaly detection. In addition, the parameter  $\bar{\tau}$  was determined as 10 s by following opinions from clinical epilepsy specialists.

### D. Seizure Prediction

All preictal episodes and all interictal episodes that were not used for modeling were monitored by following Algorithm 2 for validation. The numbers of validated awakening preictal and interictal episodes were 11 and 41, respectively. The total length of the validated interictal episodes was 38.4 h. In this

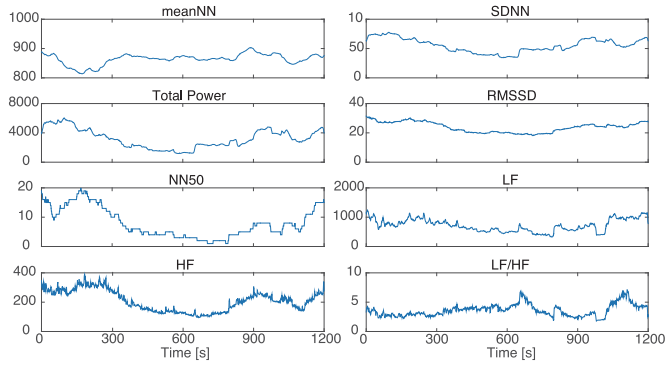


Fig. 7. HRV features derived from A2.

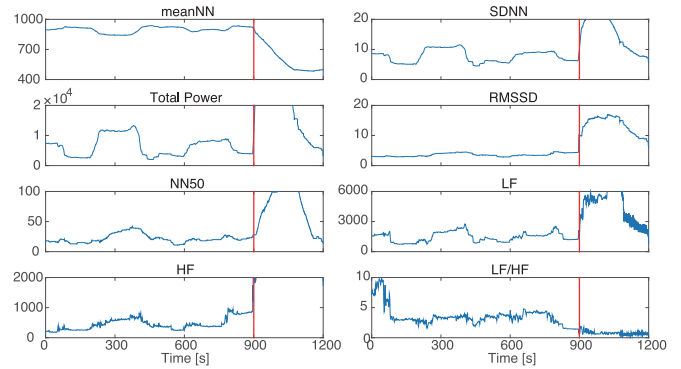


Fig. 10. HRV features derived from Is1.

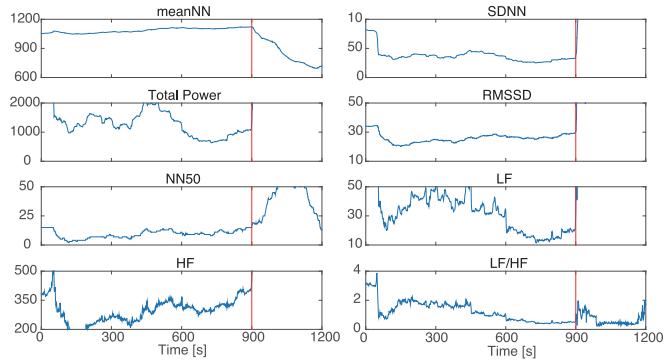


Fig. 8. HRV features derived from As3.

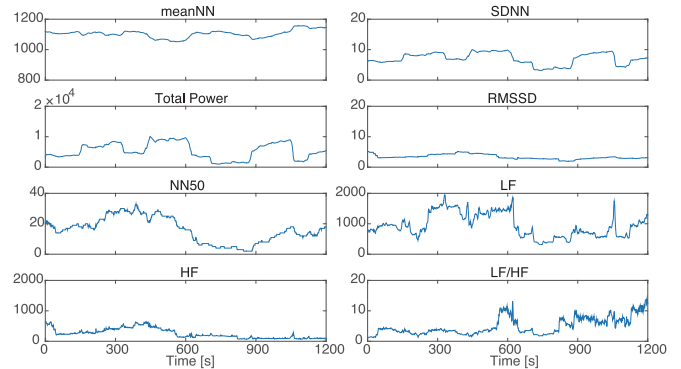


Fig. 11. HRV features derived from M2.

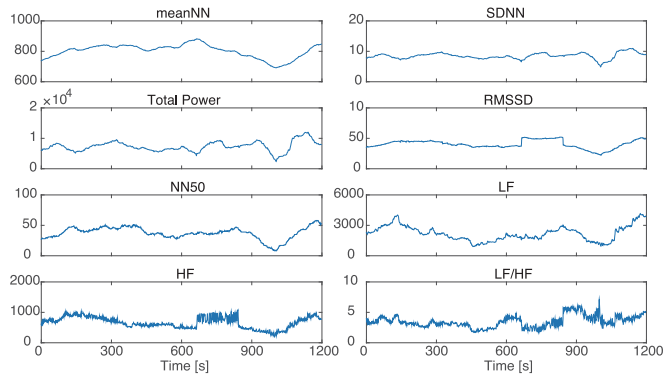


Fig. 9. HRV features derived from I3.

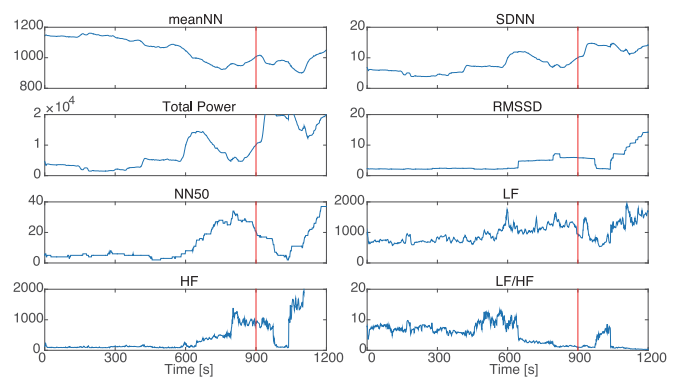


Fig. 12. HRV features derived from Ms2.

paper, seizure prediction success means that a seizure can be predicted from 15 min before to just before the seizure onset.

Monitoring results of preictal episodes As3, Is1, Ms2, and Ns1 are shown in Figs. 15–18. In these figures, horizontal dashed lines and vertical lines express the control limits of the  $T^2$  and  $Q$  statistics and the seizure onset, respectively. A colored band denotes a preictal period discriminated by the proposed method.

According to Algorithm 2, a seizure is predicted only when either  $T^2$  and  $Q$  statistic exceeds its control limit continuously for more than  $\bar{\tau} = 10$  s. The  $Q$  statistic around 500 s in Fig. 17

was not discriminated as seizure prediction, since it did not exceed its control limit for more than 10 s continuously.

From the preictal episode results, the  $Q$  statistic could detect 10 out of 11 awakening seizures except episode Is1 as shown in Fig. 16. On the other hand, the  $T^2$  statistic could predict 6 out of 11 seizures except episodes Es1, Fs2, Is1, Js1, and Ks1. Therefore, the sensitivity of the  $T^2$  and  $Q$  statistics are 55% and 91%, respectively. In addition, the mean and the standard deviation of the first seizure prediction time [s] by the  $T^2$  and  $Q$  statistics were  $524 \pm 216$  and  $494 \pm 262$  s before seizure onsets, respectively.

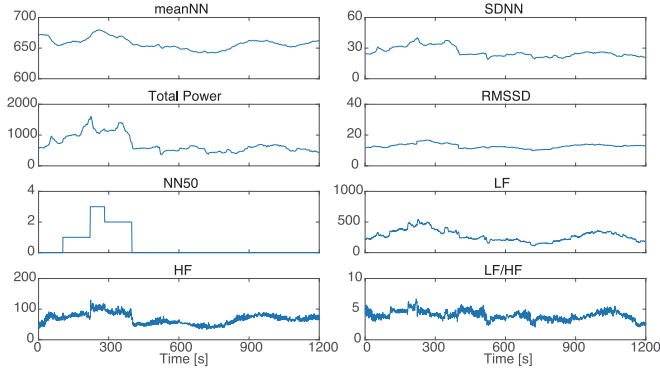


Fig. 13. HRV features derived from N2.

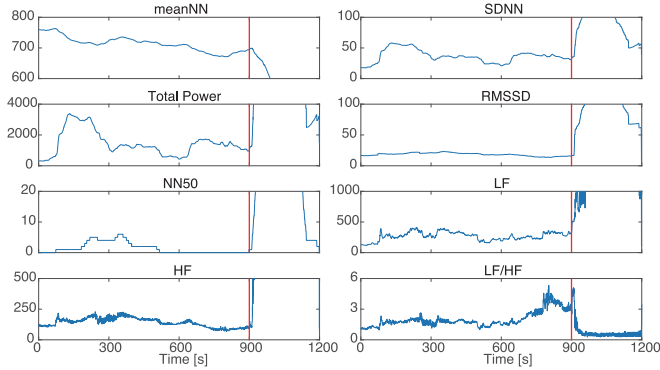


Fig. 14. HRV features derived from Ns1.

TABLE III  
INTERICTAL EPISODES USED FOR MODELING

Patient	Episodes	Length [h]	Patient	Episodes	Length [h]
A	A1	1.0	H	H1, H2	1.2
B	B1	1.5	I	I1	0.8
C	C1, C2	0.6	J	J1, J2	1.7
D	D1, D2	2.7	K	K1, K2	1.4
E	E1, E2	2.3	L	L1–L3	1.6
F	F1	0.6	M	M1	1.1
G	G1, G2	2.0	N	N1	0.4
				Total	18.9

Regarding seizures during sleep, three sleeping preictal episodes As1–As3 could be detected by both the  $T^2$  and  $Q$  statistics, while neither the  $T^2$  nor  $Q$  statistics could detect episode Bs1.

There may still be FPs in the preictal periods in which seizure detection was possible; this is because, while the epileptic neuronal activities that start in the patient brain before the clinical seizure onset can be defined as the true seizure onset, this true seizure onset is difficult to detect even if EEG data could be used.

Figs. 19–22 show prediction results of interictal episodes A2, I3, M2, and M2. There were no FPs in episodes A2 and I3; however, some FPs occurred according to the  $T^2$  statistic in episodes M2 and N2.

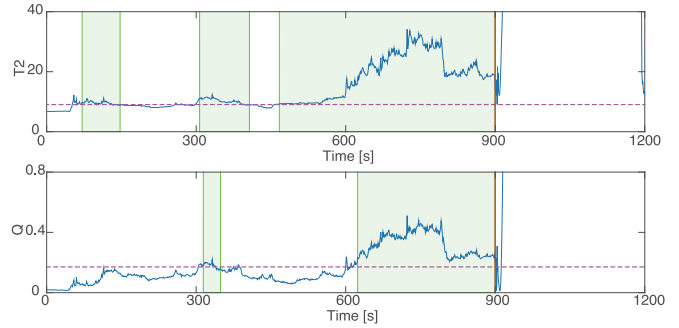


Fig. 15. Monitoring result of preictal episode As3 by MSPC.

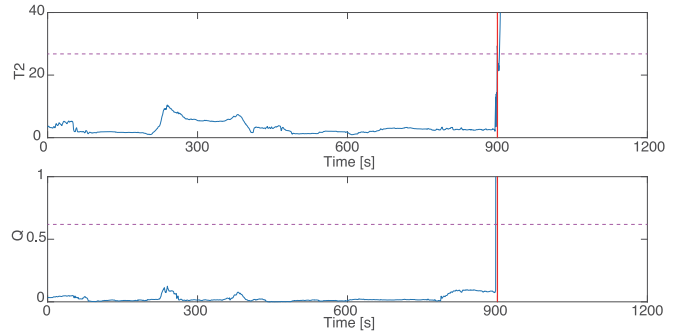


Fig. 16. Monitoring result of preictal episode Is1 by MSPC.

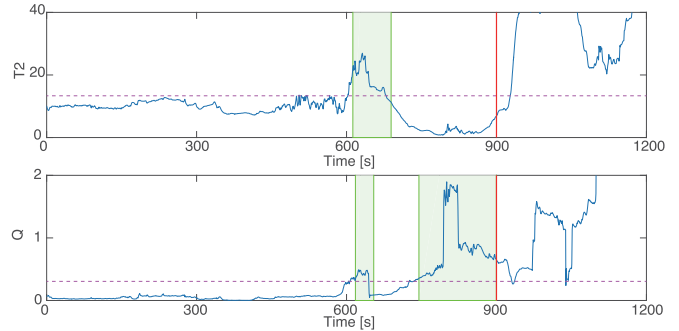


Fig. 17. Monitoring result of preictal episode Ms2 by MSPC.

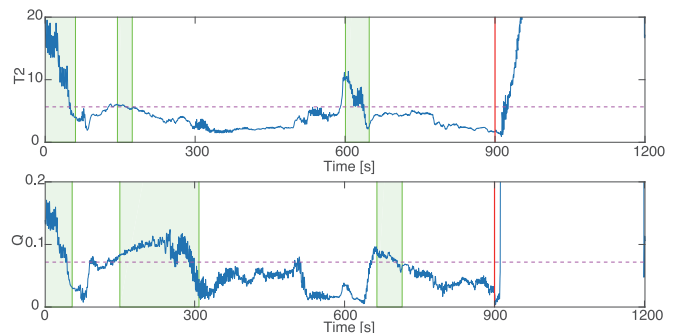


Fig. 18. Monitoring result of preictal episode Ns1 by MSPC.

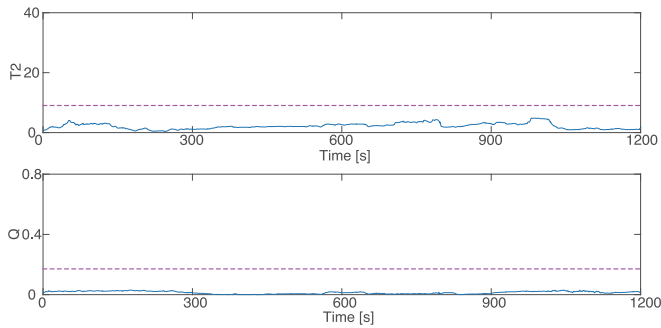


Fig. 19. Monitoring result of interictal episode A2 by MSPC.

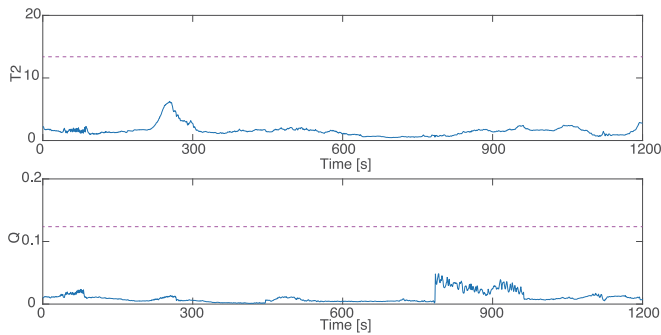


Fig. 20. Monitoring result of interictal episode I3 by MSPC.

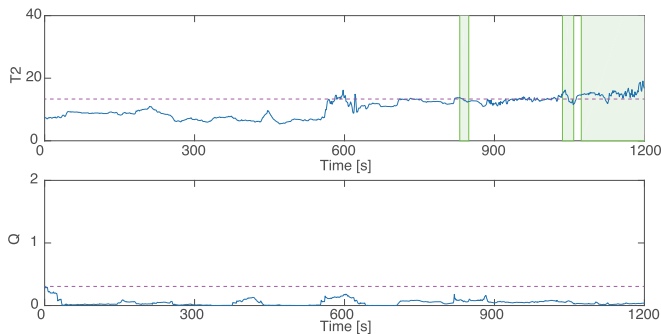


Fig. 21. Monitoring result of interictal episode M2 by MSPC.

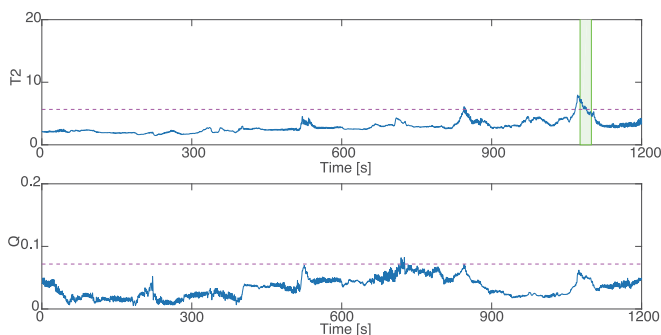


Fig. 22. Monitoring result of interictal episode N2 by MSPC.

TABLE IV  
FPS EXCEPT FOR ECG ARTIFACTS

Patient	Length [h]	$T^2$		$Q$	
		#FP	FP rate	#FP	FP rate
A	1.1	0	0	1	0.9
B	1.5	5	3.5	4	2.8
C	1.3	0	0	1	0.8
D	2.4	3	1.3	1	0.4
E	4.8	16	3.3	2	0.4
F	1.1	0	0	6	5.5
G	5.7	2	0.3	1	0.2
H	3.4	8	2.4	4	1.2
I	0.7	0	0	0	0
J	10.4	6	0.6	8	0.8
K	1.6	0	0	0	0
L	2.8	0	0	0	0
M	1.2	5	3.9	1	0.8
N	0.4	1	2.5	0	0
Total	38.4	46	1.2	29	0.7

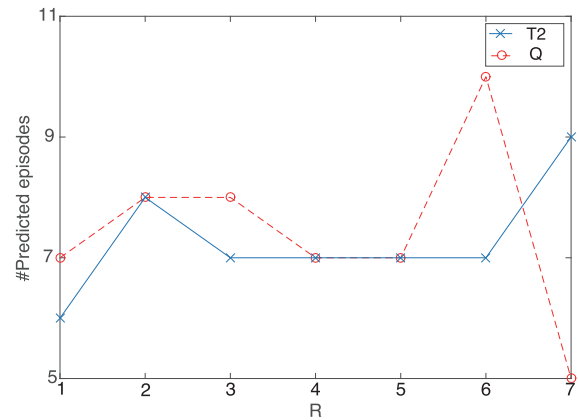


Fig. 23. Prediction performances when the number of principal components change.

Some FPs, which were caused by ECG artifacts according to the ECG data, were not used for evaluation. Table IV summarizes the number of FPs whose causes were not ECG artifacts (#FP) and FP rates. In this paper, the FP rate is defined as #FP per hour, and this evaluation is common in the field of seizure prediction [3]. The #FP in all interictal periods (total 38.4 h) by the  $T^2$  and  $Q$  statistics were 46 and 29, and the FP rates were 1.2 and 0.7 times per hour, respectively.

### E. Discussion

In this case study, the  $T^2$  and  $Q$  statistics could predict 6 and 10 out of 11 awakening seizures prior to seizure onsets, and neither the  $T^2$  nor  $Q$  statistic could predict preictal episode Is1. According to the video data of episode II that was used for modeling, patient I walked around in the hospital room and ate something. On the other hand, he rarely moved in bed while other episodes were recorded. That is, his conditions were completely different between the modeling data and the validation data, and MSPC did not function well. This result indicates that

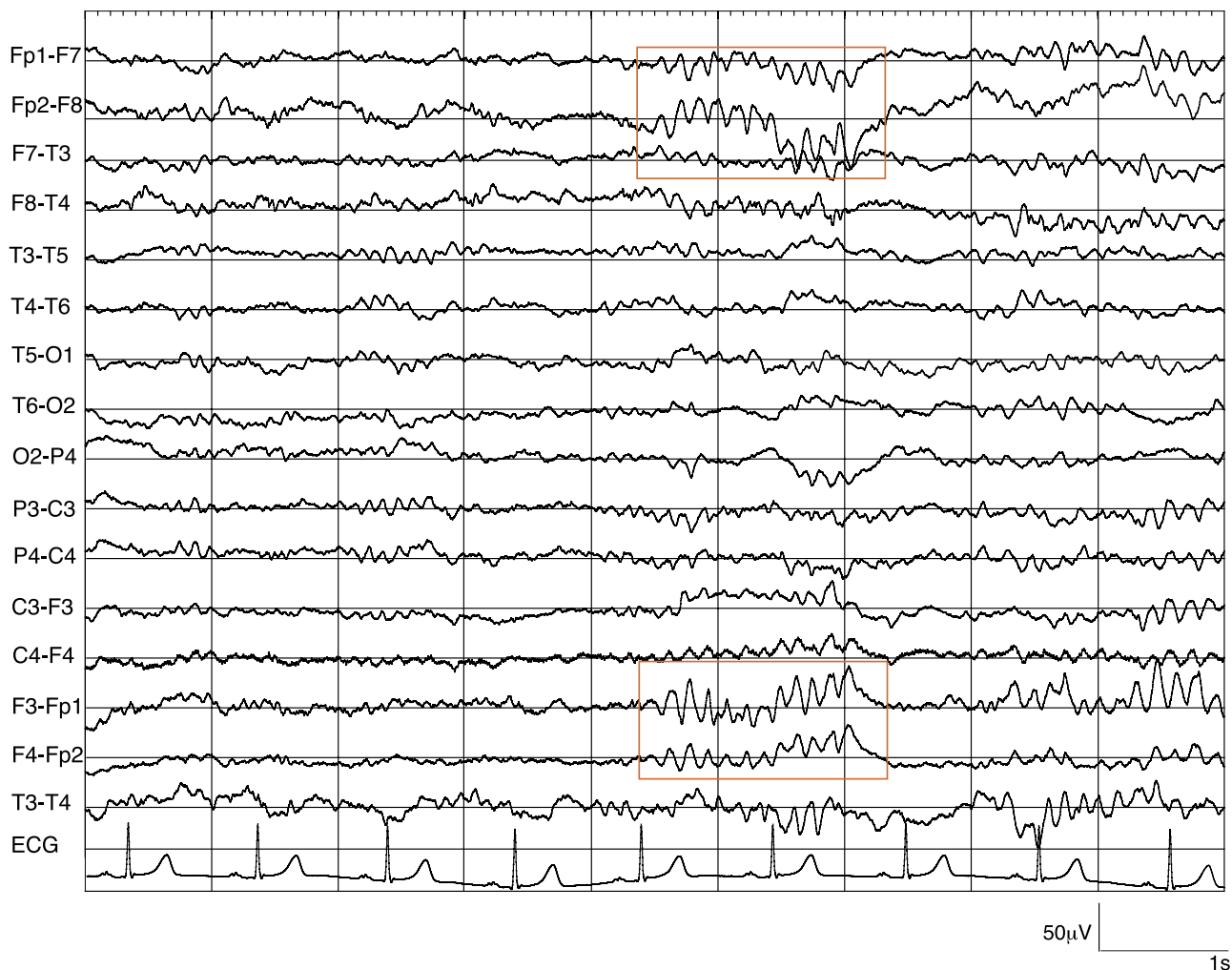


Fig. 24. Interictal paroxysmal rhythmic  $\theta$  activity over the bilateral frontal pole area in episode Bs3.

modeling data should be selected carefully for constructing a highly accurate seizure prediction model.

Whether the proposed method can predict seizures during sleep or not was validated. In this case study, three out of four interictal episodes during sleep could be predicted, which shows that the proposed method cannot always cope with seizures during sleep because the modeling data did not contain sleeping interictal data.

The interictal epileptiform discharges corresponding to the increase of the  $T^2$  and  $Q$  statistics were observed. Fig. 24 shows the interictal paroxysmal rhythmic  $\theta$  wave over the bilateral frontal pole area, which corresponds to the first seizure detection by the  $T^2$  statistic around 100 s in the prediction result of preictal episode As3 (see Fig. 15). In addition, an interictal sharp wave over the right frontal and the central area corresponding to the second seizure detection by the  $T^2$  statistic around 500 s in the prediction result of preictal episode As3 was observed. Actually, Fig. 8 shows that HRV features suddenly changed around these interictal discharges.

Although Table IV shows that the FP rate of patient F by the  $Q$  statistic was particularly high, epileptiform discharges occurred

frequently during the interictal period, and six out of nine FPs in interictal episodes of patient F seemed to correspond to them. Fig. 25 shows an example of the interictal paroxysmal rhythmic  $\delta$  waves associated with spikes over frontal, central, and parietal area with left hemisphere dominance in episode F3. Although other interictal discharges corresponding to the increase in  $T^2$  and  $Q$  statistics were not observed, these correspondences between seizure prediction and interictal discharges support the validity of the proposed method. These results agree with the previous study which suggests the influence of interictal discharges on HRV [29].

In order to validate the effect of the use of the normalized frequency domain features, the prediction performance of the seizure prediction model using LFnu and HFnu was compared with that of the model using original LF and HF. The latter model could predict 5 and 7 out of 11 seizures, and its prediction performance was inferior to the former. That is, it is important to consider HRV individuality among patients for seizure prediction.

In addition, the number of principal components  $R$  adopted for the seizure prediction model was validated. The prediction



Fig. 25. Interictal paroxysmal rhythmic  $\delta$  waves associated with spikes over frontal, central, and parietal area with left hemisphere dominance in episode F3.

performances when  $R$  changed from one to seven is shown in Fig. 23. In this figure, the horizontal and vertical axes denote the number of principal components  $R$  and the number of awakening preictal episodes whose seizure could be predicted, respectively. This result shows that the prediction performance of the  $Q$  statistic changed greatly between  $R = 5$  and 7 while that of the  $T^2$  statistic did not change much.

Table IV shows that the  $T^2$  statistic caused more FPs than the  $Q$  statistic in most patients. The seizure prediction model was constructed by using the video-EEG monitoring data for presurgical tests, and patients rarely moved in bed while the data were recorded. The FPs may have been caused by patient body motion affecting HRV. The number of principal components  $R$  was six while the number of HRV features used in this analysis was eight. Their cumulative proportion  $P_r$  of the adopted principal components reached more than 90%. In general, most of the large fluctuations in HRV are covered by major principal components and are represented by the  $T^2$  statistic. Thus, the  $T^2$  statistic is expected to capture the effect of patient body motion on HRV. In fact, most FPs observed in the  $T^2$  statistic coincided with patient motion according to the video.

According to Fig. 23, the seizure prediction performance of the  $Q$  statistic deteriorated when  $R = 7$  because almost all information retained in the residual subspace monitored by the  $Q$  statistic was noise. In other words, when  $R = 7$ , information

associated with epileptic seizures was contained in the  $T^2$  statistic and actually its prediction performance was improved.

The FP rates by the  $T^2$  and  $Q$  statistics were 1.2 and 0.7 times per hour, which are worse than conventional EEG-based seizure prediction methods whose FP rates are about 0.1–0.3 times per hour [4], [30]–[32]; however, the proposed HRV-based method does not restrict the patient's body because RRI can be easily measured by a wearable device [15], while the use of EEG-based methods in daily life is difficult because of the nature of EEG recording. In addition, since the computational load of the proposed method is much lighter than the EEG-based methods, it can be easily implemented into mobile computers. Furthermore, the proposed method can be used for closed-loop seizure treatment systems because of its ease of implementation.

In this study, the third-order spline was used for RRI interpolation and its resampling rate was 1 Hz for frequency domain feature extraction because fluctuation of RRI is usually less than 0.5 Hz. However it is possible that high-frequency HRV occurs due to arrhythmia or other circulatory diseases; in this case, 1-Hz RRI resampling is insufficient. The effect of the resampling rate for frequency domain feature extraction was validated. The frequency domain features were extracted using 4-Hz RRI resampling, and seizures were predicted by following the same procedure. The seizure prediction performance with the 4-Hz RRI resampling was the same as the 1-Hz RRI

resampling, which shows that 1-Hz resampling is enough for HRV-based seizure prediction. Considering implementation of the proposed method in a wearable RRI sensor [15], the amount of data should be reduced because computational resources of a microcomputer used in the sensor is limited. Therefore, the 1-Hz RRI resampling is suitable for the proposed method.

It is concluded that the proposed HRV-based seizure prediction method is more promising than the conventional EEG-based methods from the viewpoint of practical use.

## V. CONCLUSION AND FUTURE WORK

A new HRV-based epileptic seizure prediction monitoring method was proposed, by which RRI data recorded from epileptic patients were translated into HRV features, and the HRV features were monitored by MSPC. The application results to the clinical data showed that the sensitivity of the proposed method was 91%, and its FP rate was about 0.7 times per hour.

We are presently developing a mobile seizure prediction system based on a smartphone and a wearable RRI sensor. In this system, the wearable RRI sensor measures RRI data of a patient and sends them to the smartphone wirelessly. The smartphone app analyzes the received RRI data and discriminates the patient status between “interictal” and “preictal” in real time. Finally, the patient can receive a warning when the patient status becomes “preictal.” The developing system has the potential for improving QoL of epileptic patients through real-time seizure warning.

In future works, additional clinical data will be collected for improving accuracy of the seizure prediction algorithm, and the developing system will be tested in hospitals.

## ACKNOWLEDGMENT

The authors would like to thank the staff of the Department of Neurosurgery of Medical Hospital, Tokyo Medical and Dental University, the Department of Psychiatry of the National Center Hospital of Neurology and Psychiatry and Department of Epileptology, Tohoku University Hospital who provided patient data.

## REFERENCES

- [1] D. J. Thurman *et al.*, “Standards for epidemiologic studies and surveillance of epilepsy,” *Epilepsia*, vol. 52, pp. 2–26, 2011.
- [2] B. Chang and D. H. Lowenstein, “Epilepsy,” *New Engl. J. Med.*, vol. 345, pp. 1257–1266, 2003.
- [3] S. Ramgopala *et al.*, “Seizure detection, seizure prediction, and closed-loop warning systems in epilepsy,” *Epilepsy Behav.*, vol. 37, pp. 291–307, 2014.
- [4] L. D. Iasemidis, “Epileptic seizure prediction and control,” *IEEE Trans. Biomed. Eng.*, vol. 50, no. 5, pp. 549–558, May 2003.
- [5] P. R. Carney *et al.*, “Seizure prediction: methods,” *Epilepsy Behav.*, vol. 22, pp. S94–S101, 2011.
- [6] K. S. Eggleston *et al.*, “Ictal tachycardia: The head-heart connection,” *Seizure*, vol. 23, pp. 496–505, 2014.
- [7] C. Sevcencu and J. J. Struijk, “Autonomic alterations and cardiac changes in epilepsy,” *Epilepsia*, vol. 51, pp. 725–737, 2010.
- [8] K. Jansen *et al.*, “Peri-ictal ECG changes in childhood epilepsy: implications for detection systems,” *Epilepsy Behav.*, vol. 29, pp. 72–76, 2013.
- [9] G. D. Gennaro *et al.*, “Ictal heart rate increase precedes EEG discharge in drug-resistant mesial temporal lobe seizures,” *Clin. Neurophysiol.*, vol. 115, pp. 1169–1177, 2004.
- [10] K. Kato *et al.*, “Earlier tachycardia onset in right than left mesial temporal lobe,” *Neurology*, vol. 83, pp. 1332–1336, 2014.
- [11] M. Pagani *et al.*, “Power spectral analysis of heart rate and arterial pressure variabilities as a marker of sympatho-vagal interaction in man and conscious dog,” *Circ. Res.*, vol. 59, pp. 178–193, 1986.
- [12] S. Behbahani *et al.*, “Pre-ictal heart rate variability assessment of epileptic seizures by means of linear and non-linear analyses,” *Anadolu Kardiyol Derg.*, vol. 13, pp. 797–803, 2013.
- [13] G. Calandra-Buonaura *et al.*, “Physiologic autonomic arousal heralds motor manifestations of seizures in nocturnal frontal lobe epilepsy: Implications for pathophysiology,” *Sleep Med.*, vol. 13, pp. 252–262, 2012.
- [14] J. Jeppesen *et al.*, “Detection of epileptic seizures with a modified heart rate variability algorithm based on lorenz plot,” *Seizure*, vol. 24, pp. 1–7, 2015.
- [15] T. Yamakawa *et al.*, “Real-time heart rate variability monitoring employing a wearable telemeter and a smartphone,” in *Proc. Asia-Pacific Signal Inf. Process. Assoc. Annu. Summit Conf.*, Kaohsiung, Taiwan, Oct. 29, 2014–Nov. 1, 2014, pp. 1–4.
- [16] P. Nomikos and J. F. MacGregor, “Monitoring batch processes using multiway principal component analysis,” *AIChE J.*, vol. 40, pp. 1361–1375, 1994.
- [17] J. F. MacGregor and T. Kourti, “Statistical process control of multivariate processes,” *Control Eng. Pract.*, vol. 3, pp. 403–414, 1995.
- [18] M. Kano *et al.*, “A new multivariate statistical process monitoring method using principal component analysis,” *Comput. Chem. Eng.*, vol. 25, pp. 1103–1113, 2001.
- [19] A. J. Camm *et al.*, “Guidelines heart rate variability—Standards of measurement, physiological interpretation, and clinical use,” *Eur. Heart J.*, vol. 115, pp. 354–381, 1996.
- [20] R. E. Kleiger *et al.*, “Decreased heart rate variability and its association with increased mortality after acute myocardial infarction,” *Amer. J. Cardiol.*, vol. 59, pp. 256–262, 1987.
- [21] A. Malliani, “Cardiovascular neural regulation explored in the frequency domain,” *Circulation*, vol. 84, pp. 482–492, 1991.
- [22] E. Abe *et al.*, “Development of drowsiness detection method by integrating heart rate variability analysis and multivariate statistical process control,” *SICE J. Control. Meas. Syst. Integr.*, vol. 9, no. 1, pp. 001–008, Jan. 2016.
- [23] R. L. Burr, “Interpretation of normalized spectral heart rate variability indices in sleep research: A critical review,” *Sleep*, vol. 30, pp. 913–919, 2007.
- [24] J. E. Jackson *et al.*, “Control procedures for residuals associated with principal component analysis,” *Technometrics*, vol. 21, pp. 341–349, 1973.
- [25] E. Sforza *et al.*, “Cardiac activation during arousal in humans: Further evidence for hierarchy in the arousal response,” *Clin. Neurophysiol.*, vol. 111, pp. 1611–1619, 2000.
- [26] N. Gosselinaand *et al.*, “Age difference in heart rate changes associated with micro-arousals in humans,” *Clin. Neurophysiol.*, vol. 113, pp. 1517–1521, 2002.
- [27] Commission on Classification and Terminology of the International League Against Epilepsy, “Proposal for revised classification of epilepsies and epileptic syndromes,” *Epilepsia*, vol. 30, pp. 389–399, 1989.
- [28] A. Crespel *et al.*, “Proposal for revised classification of epilepsies and epileptic syndromes,” *Clin. Neurophysiol.*, vol. 111, pp. S54–S59, 2000.
- [29] M. M. Zaatreh *et al.*, “Heart rate variability during interictal epileptiform discharges,” *Epilepsy Res.*, vol. 54, pp. 85–90, 2003.
- [30] A. Shoeb and J. Gutttag, “Application of machine learning to epileptic seizure detection,” in *Proc. 27th Int. Conf. Mach. Learn.*, 2010.
- [31] M. D’Alessandro *et al.*, “Epileptic seizure prediction using hybrid feature selection over multiple intracranial EEG electrode contacts: A report of four patients,” *IEEE Trans. Biomed. Eng.*, vol. 50, no. 8, pp. 603–614, Aug. 2003.
- [32] L. D. Iasemidis *et al.*, “Adaptive epileptic seizure prediction system,” *IEEE Trans. Biomed. Eng.*, vol. 50, no. 5, pp. 616–626, May 2003.

Authors’ photographs and biographies not available at the time of publication.